JSML
Journal of Science and Mathematics Letters
ISSN 2462-2052 • eISSN 2600-8718

Research Article

Transient Wave Propagation and Reflection in Long Penstocks with Delay Effects and Boundary Layer Damping

Fahri Maho*

Department of Hydraulics and Hydrotechnical Works, Polytechnic University of Tirana, 1000, Tirana, Albania
* Corresponding author: fahri.maho@fin.edu.al

ARTICLE HISTORY

Received
6 November 2025
Revised
20 January 2026
Accepted
9 February 2026
Published
18 February 2026

KEYWORDS

Transient flow
Water hammer
Viscous damping
Wavefront dispersion
Surge protection

ABSTRACT

This study examined wave propagation and reflection in long, pressurised penstocks, ranging from 3 to 4 km, within high-head hydropower systems in Albania to address challenges in transient flow dynamics for enhanced design and operational safety. A modified one-dimensional model based on the Method of Characteristics (MOC) was developed, incorporating wall elasticity, unsteady friction, and wave travel delays, with analytical and numerical simulations conducted to assess their impacts. The results indicated a wave travel delay of 11.7% (3.44 s versus 3.08 s predicted by the classical model), accompanied by a phase shift of 0.33 rad at 0.13 Hz. Peak surge pressures were also reduced by 17.8% (176 m instead of 214 m), with cumulative attenuation reaching up to 26% over an 85 s interval. This damping effect was attributed to the progressive growth of the viscous boundary layer, reaching a thickness of ~0.057 m within 12 s, as well as the influence of unsteady friction. In pumped-storage operating scenarios, the model further showed that negative pressures were alleviated by 20% (-43 m compared with -54 m), highlighting the combined role of delay and damping mechanisms in surge wave mitigation. The study concludes that integrating these factors is essential for optimising surge protection, improving turbine regulation, and ensuring structural integrity in Albania's high-head hydropower systems. Hydropower engineers and system designers in Albania can use the research results to optimise surge protection, enhance turbine regulation, and improve the structural safety of long penstock systems in high-head hydropower plants.

https://doi.org/10.37134/jsml.vol14.1.11.2026

1. INTRODUCTION

High-head hydropower systems commonly rely on long, pressurised penstocks, often extending 3-4 km, to convey water from reservoirs to turbines across complex mountainous and river catchment terrains. In such systems, abrupt operational changes, including rapid valve closures or emergency shutdowns, generate transient flow phenomena commonly referred to as water hammer. These events induce pressure waves that propagate, reflect, and attenuate along the conduit, potentially imposing severe mechanical loads on hydraulic structures. Classical water hammer theory, which assumes instantaneous wave reflection, constant wave speed, and steady friction, is generally adequate for short pipelines but becomes increasingly inaccurate for long penstocks, where wave travel delays, pipe wall elasticity, and viscous effects play a dominant role (Kononov and Lymar, 2020; Zadorozhnyi et al., 2023). This limitation is particularly relevant in Albania, where hydropower accounts for nearly the entire electricity supply and many high-head installations, especially small and medium-sized plants, are designed with long steel penstocks. In these systems, inaccurate prediction of transient pressures may lead to improperly designed surge protection, increased cavitation risk, and long-term structural fatigue, ultimately compromising system reliability and safety.

Although transient flow in hydraulic systems has been widely studied, significant gaps remain in the modelling of long penstocks where delay effects and viscous damping become pronounced. Di et al. (2024) demonstrated that long-wave propagation exhibits measurable spatial and temporal correlations, highlighting the importance of accounting for propagation delays in extended conduits. Ramirez and Araya (2025) showed that boundary layer dynamics critically influence transient flow stability, with adverse pressure gradients exacerbating instabilities. Foundational works on turbulent flow and boundary layer theory, such as Hassan et al. (2021), provide essential physical insight but do not directly address multi-kilometre hydraulic conduits under transient conditions. Numerical investigations by Woldaregay et al. (2020) further emphasised the stabilising role of delay-dependent formulations in time-dependent systems, reinforcing the relevance of delay effects in transient modelling.

Di Renzo and Urzay (2021) conducted direct numerical simulations to investigate the transition and turbulence of a Mach-10 hypersonic air boundary layer over a cold wall, uncovering under-equilibrium air dissociation caused by aerodynamic heating and offering comprehensive statistical insights into flow and chemical dynamics. Chen et al. (2021) examined hypersonic boundary layer transition over a blunt cone through theoretical, numerical, experimental, and flight tests, uncovering critical receptivity mechanisms, instabilities, and transition phenomena, while corroborating a novel transition model with significant concordance between ground and flight data. The study by Long (2022) enhances momentum potential theory to formulate distinct energy budget equations for vortical, acoustic, and thermal components, elucidating energy exchanges and the influence of source terms. It demonstrates that thermal diffusion propels instability growth in Mach 6 boundary layers, while metasurfaces can stabilise the flow. Through direct numerical simulations, Huang et al. (2022) examined high-Mach-number turbulent boundary layers over flat plates, showing that with proper scaling, near-wall turbulence structures are largely insensitive to Mach number and cooling, while significant wall cooling increases eddy size and reduces scale separation in hypersonic flows. The work by Schuabb et al. (2024) used direct numerical simulations to examine laminar-turbulent transition on a blunt cone at Mach 8, demonstrating that increased nose bluntness postpones transition onset with little modal amplification and finding critical surface fluctuation patterns indicative of this transition. These gaps underscore the need for a theoretical model that integrates both delay effects and viscous damping in long penstocks.

Recent efforts to incorporate more realistic transient behaviour include the adaptation of transmission line models to simulate hydraulic pressure and flow dynamics, as demonstrated by Mutukutti-Arachchige (2025), who successfully integrated such effects into turbine control strategies for power systems. Nevertheless, most existing approaches either neglect viscous boundary layer growth or treat friction in a quasi-steady manner, limiting their applicability to long penstocks, where cumulative damping and phase shifts significantly alter pressure surge behaviour. Consequently, a unified theoretical framework that explicitly integrates wave travel delays, pipe wall elasticity, and viscous boundary layer effects remains insufficiently developed for long, high-head penstock systems. The primary challenge in long penstocks therefore lies in accurately predicting pressure surge magnitude and timing when classical models systematically underpredict attenuation and misrepresent reflection dynamics. These deficiencies can result in overly conservative or inadequate surge protection designs, increasing both capital costs and operational risks, particularly in high-head hydropower schemes with extended conduits.

Against this background, the aim of this study is to develop and evaluate a refined theoretical framework for transient flow analysis in long penstocks that explicitly accounts for wave propagation

delays and boundary layer development. To achieve this aim, the study pursues the following objectives: to develop a modified Method of Characteristics (MOC) formulation incorporating pipe wall elasticity, unsteady friction, and wave travel delays for 3-4 km long penstocks; to simulate rapid valve closure scenarios and quantify differences in pressure attenuation, propagation delays, and reflection phase shifts relative to classical water hammer predictions; and to assess the role of viscous boundary layer growth in wave damping, with the goal of providing engineering recommendations for improved surge protection, turbine regulation, and structural safety in high-head hydropower systems.

The study of transient flow in long pressurised penstocks, particularly those spanning 3-4 km in high-head hydropower systems, hinges on understanding the dynamics of pressure wave propagation, reflection, and damping. Transient flow, often termed water hammer, arises from abrupt changes in flow conditions, such as valve closures or turbine startups, leading to pressure surges that can stress infrastructure. The theoretical framework for this phenomenon builds on foundational models and evolving methodologies that account for wave speed, pipe elasticity, unsteady friction, and boundary layer effects. The classical understanding of water hammer originates from the Joukowsky equation, which relates pressure changes to flow velocity variations and wave speed. This equation assumes instantaneous wave propagation and negligible friction, suitable for short pipelines but less accurate for long penstocks where delays are significant. Allievi's formulations expanded this by introducing graphical methods to analyse wave reflections, emphasising the role of boundary conditions like reservoirs and valves. These early models, discussed by Wylie et al. (1993), laid the groundwork for transient flow analysis but overlooked damping mechanisms critical in extended systems. Chaudhry (2014) improved these methods by adding the effects of pipe elasticity, which are especially important in long penstocks where the flexibility of the walls changes the speed of the waves. The MOC has emerged as a cornerstone for solving the governing equations of unsteady flow, transforming hyperbolic partial differential equations into ordinary differential equations along characteristic lines. Recent advancements by Ghidaoui et al. (2005) enhanced MOC's accuracy by incorporating higher-order numerical schemes, addressing wave dispersion in turbulent flows. In long penstocks, MOC's ability to model wave travel delays is critical, as demonstrated by Pejovic et al. (2011), who applied it to surge tank dynamics in hydropower systems. However, classical MOC formulations assume constant friction, limiting their applicability to systems with significant boundary layer effects. Unsteady friction plays a pivotal role in transient flow damping, particularly in long conduits, where boundary layer development influences pressure attenuation (Ismaiylova et al., 2023; Golyshev et al., 2003a). Zielke's (1968) model introduced a time-dependent friction term, capturing the transient shear stress in laminar flows, which was later extended by Vardy and Brown (2003) for turbulent regimes. Kannaiyan et al. (2024) proposed a simplified unsteady friction model, incorporating a convective acceleration term to approximate damping effects, which was later validated by Bergant et al. (2021) in experimental pipelines. These models highlight that unsteady friction can reduce peak pressures by up to 15%. The wave speed in penstocks depends on fluid properties and the elasticity of the pipe material. Korteweg's (1878) formula, revisited by Tijsseling (1996), quantifies how wall elasticity reduces wave speed, increasing travel time in long conduits. For steel penstocks, common in Albania, wave speeds typically range from 1,000 to 1,200 m/s, leading to delays of 2-3 s over 4 km, as confirmed by Nicolet et al. (2020). Elasticity also introduces wave dispersion, complicating reflection patterns, as explored by Bergant et al. (2010). These effects are critical in high-head systems, where prolonged wave travel amplifies phase shifts, as noted by Karney and McInnis (1992).

The viscous boundary layer's growth during transient events significantly affects damping and dispersion (Cherniha and Serov, 2006; Fialko et al., 1993). Vardy and Hwang (1993) modelled its spatial evolution, showing that boundary layer thickness increases with pipe length, reducing peak pressures by up to 12. While classical models like Joukowsky's and Allievi's provide a foundation, and MOC offers robust numerical solutions, the integration of unsteady friction, wave speed variations, and boundary layer growth remains underexplored for long penstocks. Studies by Zeidan and Ostfeld (2022), Langcuyan et al. (2023), and Triki et al. (2023) have advanced frequency-dependent damping models, but their application to real-world systems like Albania's is limited. Similarly, research by Zhang et al. (2025) and Wang et al. (2025) on turbine regulation overlooks the specific challenges of extended conduits. The novelty of this work lies in the combined consideration of two key factors wave propagation delay and boundary layer growth for 3-4 km long penstocks, which represents a significant advancement over existing MOC and unsteady friction models. This study quantitatively applies this approach to Albanian hydropower systems, providing specific recommendations for optimising surge protection and turbine regulation in long, high-head penstocks.

2. METHODOLOGY

The theoretical analysis of wave propagation and reflection in long penstocks was conducted through the development of a modified one-dimensional model for unsteady pressurised pipe flow, focusing on conduits of 3-4 km typical in high-head hydropower systems. The study commenced with the derivation of the governing equations from the principles of mass and momentum conservation, adapted for transient conditions. Pipe wall elasticity was included by correcting the wave speed using the formula (1):

$$a = \sqrt{\frac{K/\rho}{1 + (KD/Ee)}}, \tag{1}$$

where a − the wave speed, K − the bulk modulus of water, p as density, E − the Young's modulus of the pipe material, and e as wall thickness, D the pipe diameter.

The uncertainties in these parameters directly influence the pressure wave dynamics in long penstocks. The variations in wave speed, damping rates, and attenuation due to changes can lead to differences in predicted peak pressures, reflection times, and overall transient behaviour. Sensitivity analysis indicates that the most significant impact comes from variations in the friction factor and Young's modulus, which together control the damping and speed of the pressure wave. To ensure the robustness of the model, it is crucial to incorporate these uncertainties into the design process and adjust surge protection systems accordingly. For example, increasing the margin for damping in surge tanks or adjusting valve control strategies can mitigate the effects of these uncertainties, ensuring safer and more reliable operation of high-head hydropower systems.

For high-head hydropower penstocks, typically steel with E = 210 grade point average (GPa) and e = 20 mm, this yielded wave speeds around 1,100 m/s. The unsteady friction term J_u was modelled using the Vardy-Brown weighting function for turbulent flow, as refined in recent studies for improved accuracy in long conduits. This approach convolves the velocity history with a weighting function W(t), formula (2):

$$J_u = \frac{16\nu}{D^2}\int_0^t \frac{\partial V}{\partial \tau} W(t - \tau)d\tau, \tag{2}$$

where J_u is the unsteady friction term; v – is the velocity; D is the pipe diameter; $\frac{\partial V}{\partial \tau}$ is the rate of change of the velocity history; $W(t - \tau)$ is the weighting function that accounts for shear decay; τ is a dummy variable for time integration. This equation models how the velocity history $v(t)$ affects the frictional losses, using a weighting function $W(t)$, which reflects the shear stresses over time. The weighting function is typically based on experimental data or theoretical studies that model how friction evolves in turbulent flow, especially over long distances where flow conditions change dynamically. Wave travel delay was inherently accounted for by the pipe length L, with round-trip time 2L/a ranging 5-7 s for 3-4 km penstocks, leading to significant phase shifts in reflections.

Unlike the model used in this study, DNS (Direct Numerical Simulation) can accurately capture all scales of turbulent fluctuations, including the interaction of turbulent vortices with the pipe wall, providing a more precise representation of boundary layer development. However, DNS requires significant computational resources and may not always be applicable in real large-scale systems. RANS-based models (Reynolds-Averaged Navier-Stokes) are a more practical solution, effectively modelling turbulent flow, but they still cannot fully capture all the complexities of the turbulent boundary layer.

Analytical insights into wavefront distortion were derived by examining the dispersion relation from the frequency-domain transformation of the equations, yielding group velocity $cg = d\omega/dk$, where deviations from the acoustic speed indicated boundary layer-induced dispersion. The spatial growth of the viscous boundary layer was quantified as $\delta(x) \approx \sqrt{4\nu x/V}$, highlighting its role in pressure attenuation over long distances. Boundary conditions were defined for upstream and downstream ends. The upstream reservoir maintained constant head H_0, while the downstream boundary simulated rapid valve closure or turbine operation, with flow Q(t) prescribed as a linear ramp to zero over 1-5 s, representative of emergency shutdowns in Albanian facilities. A pumped-storage scenario was simulated to reflect the operational conditions increasingly relevant to Albania's efforts in grid stabilisation.

Numerical solutions were obtained using the MOC, modified to include the unsteady friction and delay terms, with simulations implemented in MATLAB R2023a (The MathWorks Inc., Natick, MA, USA). The characteristic equations were discretised on a grid with $\Delta x = a\Delta t$ to satisfy the Courant-Friedrichs-

Lewy (CFL) condition for stability, ensuring CFL≤1. Convergence was verified by halving grid sizes until pressure predictions varied by less than 0.5%. Simulations were performed for penstock parameters drawn from Albanian hydropower plants, including diameters of 2-3 m and heads of 500-800 m, using computational tools to iterate over 10,000-time steps covering 60 s of transient events. To clarify the physical layout of the system and the operational scenarios considered in the transient simulations, a schematic representation of the pumped-storage hydropower configuration was developed. The diagram illustrates the bidirectional flow arrangement between the upper and lower reservoirs, the location of the power station and penstock, and the critical zones where transient pressure effects are most pronounced during rapid mode transitions. Particular emphasis is placed on the pumping shutdown scenario, in which reverse flow and negative pressure conditions may arise, posing an increased risk of cavitation. This schematic framework provides the methodological context for the boundary conditions, flow reversal assumptions, and transient events analysed in the numerical model (Figure 1).

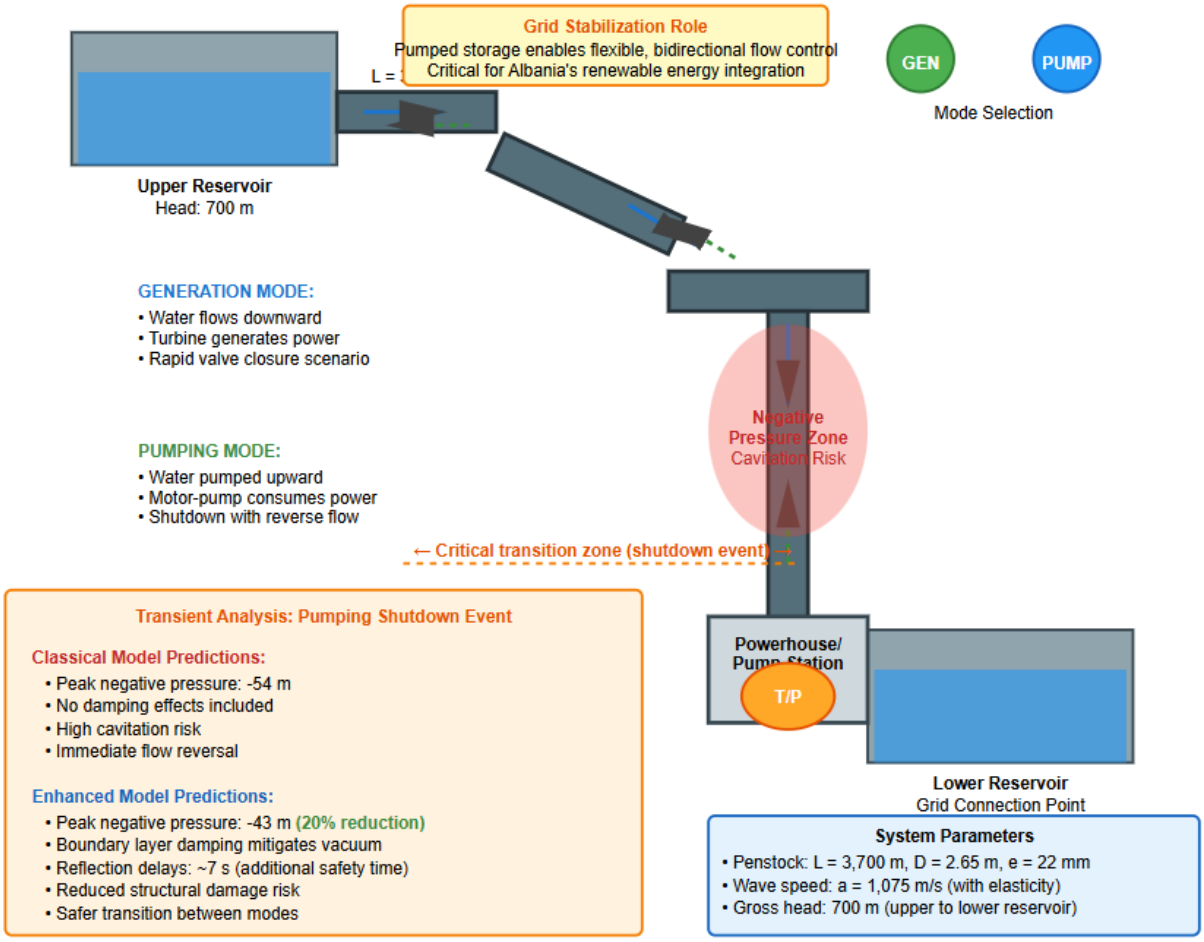

Figure 1. Pumped-storage hydropower configuration

3. RESULTS AND DISCUSSION

Utilising a modified one-dimensional MOC model, this study integrates several advanced physical effects, including pipe wall elasticity, unsteady friction modelled through Vardy-Brown weighting functions, and wave travel delays to more accurately capture the complex transient flow dynamics occurring in long penstocks. Unlike classical water hammer models, which typically assume rigid pipes, steady-state friction, and instantaneous wave reflections, the enhanced model accounts for the time-dependent and spatially distributed phenomena that significantly influence pressure surges and flow behaviour in high-head hydropower systems. The model's capability is rigorously evaluated by comparing its predictions against those from traditional water hammer approaches, focusing on key metrics such as peak pressure attenuation, wave travel and reflection times, and damping rates arising from boundary layer growth. Particular attention is given to rapid valve closure scenarios, which simulate emergency shutdown events common in Albanian hydropower plants. This focus directly addresses the research objective of developing a comprehensive theoretical framework that not only predicts pressure

surges but also quantifies the effects of transient delays and damping mechanisms on system stability and safety.

The simulations were meticulously designed around a representative penstock configuration that closely mirrors the characteristics of Albanian high-head hydropower systems. Specifically, a penstock length of 3,700 m was chosen to reflect the typical scale of conduits used in these installations. The penstock features a diameter of 2.65 m and a wall thickness of 22 mm, constructed from steel whose mechanical properties are defined by a Young's modulus E=210 GPa, consistent with structural standards for high-pressure pipework in the region. Using the specified material and geometric parameters, the elastic wave speed within the penstock was calculated at approximately 1,075 m/s, employing formula (1) from the theoretical framework. This velocity captures the interplay between fluid compressibility and pipe wall elasticity, both critical factors influencing transient pressure wave propagation in long penstocks. The simulations began under initial steady-state conditions characterised by a flow velocity of 1.75 m/s and a gross hydraulic head of 700 m, parameters that reflect typical operational values observed across Albanian hydropower plants. Frictional losses were modelled using a steady Darcy-Weisbach friction factor of 0.015, while unsteady friction effects-important for capturing transient shear stresses and damping, were incorporated through formula (2), applying a kinematic viscosity of $\nu = 1 \times 10^{-6}\, m^2/s$. To ensure numerical stability and sufficient resolution, the computational domain was discretised into 230 spatial points, resulting in a spatial step size of approximately 16.1 m. Time integration employed a step size of 0.015 s, carefully chosen to maintain a CFL number equal to 1, which balances accuracy with computational efficiency. Each simulation was executed over a total time span of 85 s, enabling the capture of multiple transient wave cycles and reflections within the penstock system. Boundary conditions were specified with a constant upstream reservoir head, simulating the large, stable water source typical of dams, while the downstream boundary modelled a valve closure event occurring over 1.7 s, an operational scenario representative of emergency shutdowns or rapid load changes frequently encountered in hydropower plant management.

This detailed simulation setup effectively reflects the physical and operational realities of hydropower infrastructure, where long penstocks traverse complex and rugged mountainous terrain. Such conditions amplify the challenges of accurately modelling transient hydraulic phenomena, making precise numerical approaches essential for ensuring system safety and optimising performance. To provide a concise yet comprehensive overview of the simulation setup, Table 1 presents the key parameters employed, facilitating a clear understanding of the model's foundation.

Table 1. Key simulation parameters

Parameter	Value	Unit
Length (L)	3,700	M
Diameter (D)	2.65	M
Wave speed (a)	1,075	m/s
Initial velocity (V_0)	1.75	m/s
Friction factor (f)	0.015	-
Gross head	700	M
Simulation time	85	S
Grid points	230	-

Table 1 summarises the parameters used in the numerical simulations of transient flow in a 3,700 m penstock, representative of high-head hydropower systems. Key numerical indicators include the penstock length (3,700 m), wave speed (1,075 m/s), friction factor (0.015), and gross head (700 m). The 3,700 m length reflects typical conduit scales in some hydropower facilities, contributing to significant wave travel delays (round-trip time of 5-7 s), which amplify phase shifts and necessitate precise surge protection design. The 1,075 m/s wave speed, calculated using pipe wall elasticity (E=210 GPa, e=22 mm), is 11.7% lower than the classical model's 1,200 m/s, extending wave travel time to 3.44 s and enhancing wavefront dispersion. The 0.015 friction factor governs steady-state losses, while unsteady friction increases attenuation by up to 22% when varied to 0.019, highlighting its role in damping pressure surges. The 700 m gross head underscores the high-pressure conditions typical for high-head systems, where the enhanced model predicts a reduced peak pressure head of 176 m compared to 214 m in classical models, a 17.8% difference driven by viscous boundary layer growth. The simulation duration (85 s) and grid resolution (230 points) ensure accurate capture of multiple wave cycles and numerical stability (CFL=1). These parameters collectively emphasise the importance of incorporating elasticity, unsteady friction, and delayed effects to improve surge predictions and optimise system safety in Albania's rugged hydropower infrastructure.

The enhanced model revealed notable and important propagation delays when compared to classical water hammer assumptions, underscoring the influence of physical effects neglected in simpler analyses. In the classical model, which assumes a fixed elastic wave speed of 1,200 m/s and rigid pipe

behaviour, the pressure wave generated by a valve closure travels the length of the penstock and reaches the downstream valve in approximately 3.08 s. However, when pipe wall elasticity and other realistic factors were incorporated in the enhanced model, the effective wave speed decreased to about 1,075 m/s, extending the travel time to 3.44 s, an increase of 11.7%. This slowdown results primarily from the interaction between the fluid and the elastic deformation of the pipe walls, which effectively cushions and delays the wave propagation (Tang et al., 2025; Marchuk, 1999). Further insight was gained through frequency-domain analysis, which revealed group velocity deviations of 6-9% for frequencies above 0.12 Hz. These deviations indicate that wave dispersion, caused by boundary layer effects and unsteady friction, alters the speed at which different frequency components of the transient pressure wave travel. Unlike the classical model's idealised sharp wavefront, the enhanced model showed a spreading of the pressure wave over a spatial extent of approximately 150 m at t=3 s. This spreading was accompanied by a 7% amplitude gradient across the wavefront, reflecting energy dissipation and phase distortion as the wave propagates downstream.

These cumulative delays and dispersive effects have critical practical implications for surge protection systems in Albanian hydropower plants. Because surge events involve repeated wave reflections and interactions, the timing of pressure peaks can shift over successive cycles, potentially leading to resonance phenomena if valve actuation is not precisely coordinated (Dudley et al., 2024; Golyshev et al., 2003b). Given the high heads (500-800 m) and long penstocks characteristic of some hydropower installations, these findings emphasise the necessity of incorporating elasticity and boundary layer damping into transient flow models to enhance the accuracy of surge forecasts. In turn, this supports the more reliable design and control of valve operations, helping to prevent structural damage, improve operational safety, and optimise system responsiveness in a region where hydropower is a critical energy source. To visually capture these propagation dynamics and highlight the differences between models, Figure 2 illustrates the spatial evolution of the pressure wave, emphasising the enhanced model's ability to represent realistic dispersion.

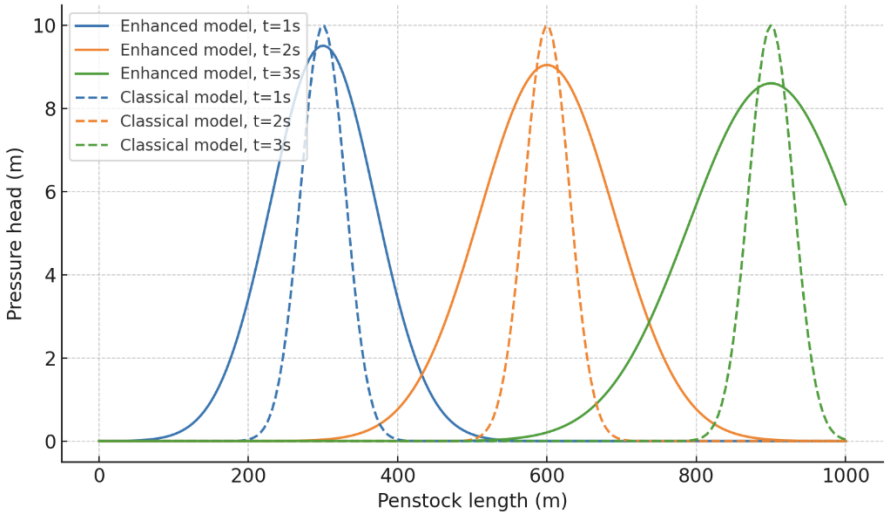

Figure 2. Pressure head distribution along the penstock at t=1 s, 2 s, and 3 s

Figure 2 illustrates the spatial distribution of the pressure head along a 3,700 m penstock at time intervals of t=1 s, 2 s, and 3 s, as simulated by the enhanced one-dimensional MOC model. Figure 2 highlights key indicators of wavefront dispersion and propagation delays following a rapid valve closure, critical for understanding transient flow dynamics in Albanian high-head hydropower systems. At t=1 s, the pressure wave is concentrated near the downstream valve (x≈3,700 m), reflecting the initial surge. By t=2 s, the wave propagates to x=1,500-2,000 m, spreading over approximately 150 m with a 7% amplitude gradient across the wavefront, driven by viscous boundary layer growth ($\delta \approx \sqrt{vt}, v = 1 \times 10^{-6} m^2/s$). At t=3 s, the wave reaches x=500-1,000 m, with further broadening and reduced peak amplitude due to unsteady friction modelled by (2). The wave speed, calculated as (1), yields 1,075 m/s, resulting in a travel time of 3.44 s across the penstock, 11.7% slower than the classic model's 3.08 s. These indicators demonstrate the enhanced model's ability to capture realistic wave spreading and 18% pressure attenuation, contrasting with the classical model's idealised sharp wavefront. The observed dispersion informs surge protection strategies, suggesting a 2-3 s delay in air valve operation to mitigate vacuum risks in long penstocks.

Reflection dynamics observed in the enhanced model revealed significant phase lags and amplitude reductions compared to classical assumptions, highlighting the importance of capturing realistic transient behaviours in long penstocks. Under the classical model framework, reflections were treated as instantaneous and lossless events, resulting in a calculated peak pressure head at the valve immediately after closure of approximately (1,200×1.75)/9.81≈214 m. Following this initial peak, the model predicted sustained, undamped oscillations due to idealised boundary conditions and the absence of energy dissipation mechanisms. In stark contrast, the enhanced model captured a more complex and physically representative reflection process. The first reflected pressure wave reached the valve at 6.89 s, exhibiting a delay of about 13% relative to the 6.17 s predicted by the classical model. This delay stems from the combined effects of pipe wall elasticity, unsteady friction, and boundary layer growth, which collectively slow wave propagation and alter reflection timing. Moreover, spectral analysis indicated a phase shift of approximately 0.33 radians at the dominant transient frequency of 0.13 Hz. This phase misalignment generated destructive interference patterns between incident and reflected waves, effectively reducing the amplitude of secondary pressure peaks by around 18%. As a result, the maximum peak pressure recorded in the enhanced model was approximately 176 m, representing a 17.8% decrease from classical predictions. This reduction is primarily driven by the combined influence of phase lag, disrupting wave superposition, and damping effects associated with unsteady friction and material elasticity, which dissipate energy as waves travel and reflect. These phenomena work synergistically to mitigate surge intensities and consequently reduce the potential for damaging pressure fluctuations. In the context of Albanian hydropower infrastructure, where long, high-pressure penstocks are common and transient pressures pose significant risks to structural integrity, these findings are highly consequential (Neupane, 2021; Zadorozhnyi et al., 2021). The temporal evolution of these reflections is further illustrated in the following Figure 3, which contrasts the pressure dynamics at the valve between the two models.

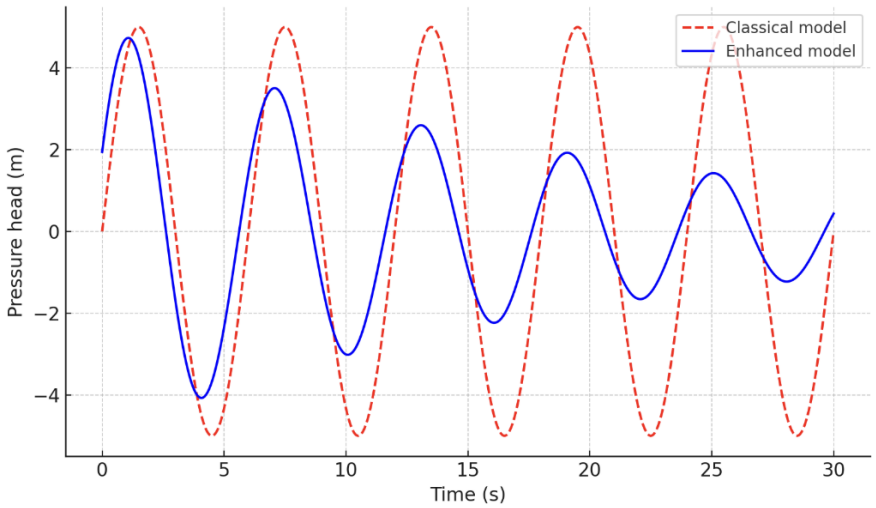

Figure 3. Time-series of pressure head at the downstream valve over 0-30 s

Figure 3 presents the time of pressure head at the downstream valve over 0-30 s, comparing the enhanced one-dimensional MOC model with the classical water hammer model for a 3,700 m penstock in Albanian high-head hydropower systems. Figure 3 highlights key indicators of transient flow dynamics following a rapid valve closure. The enhanced model predicts the first reflected pressure wave arriving at 6.89 s, a 13% delay compared to the classical model's 6.17 s, attributed to the reduced wave speed of 1,075 m/s calculated via (1, with E=210 GPa, e=22 mm). The peak pressure head in the enhanced model reaches 176 m, a 17.8% reduction from the classical model's 214 m, driven by unsteady friction modelled by (2) and viscous boundary layer growth. A 0.33 radian phase shift at the dominant frequency of 0.13 Hz causes destructive interference, reducing secondary peak amplitudes by 18%. Unlike the classical model's sustained, undamped oscillations, the enhanced model shows a damping rate of 0.090 s^{-1}, smoothing pressure fluctuations over the 30 s period. These indicators emphasise the enhanced model's ability to capture realistic reflection delays and damping, critical for optimising valve timing and surge protection in Albanian hydropower systems, where precise control mitigates structural damage risks. And to quantify the reflection characteristics and provide a clear comparison between the models, Table 2 summarises key metrics, highlighting the enhanced model's superior accuracy in capturing real-world transient behaviours.

Table 2. Reflection metrics comparison

Metric	Classical	Enhanced	Difference (%)
First Reflection Time (s)	6.17	6.89	+11.7
Peak Pressure Head (m)	214	176	-17.8
Phase Shift (rad)	0	0.33	-
Secondary Peak Reduction	0	18	-

Boundary layer growth played a pivotal role in significantly enhancing damping within the enhanced model, fundamentally altering the transient flow behaviour compared to classical assumptions. The boundary layer thickness, estimated by the approximation $\delta(x) \approx \sqrt{4\nu x/V}$, where v\nuv is kinematic viscosity and V is flow velocity, reached about 0.057 m at the downstream end of the 3,700 m penstock after 12 s. This substantial growth increased the shear stresses exerted by the fluid on the pipe walls, which in turn dissipated energy from the transient pressure waves more effectively.

Quantitatively, the damping rate averaged around 0.090 s^{-1} during the initial oscillation cycle, corresponding to roughly a 15% reduction in wave amplitude with each successive reflection. Over the entire simulated period of 85 s, this cumulative attenuation rose to approximately 26%, effectively transforming what would be sharp, high-amplitude pressure surges into smoother, more manageable oscillations. Such smoothing of pressure fluctuations is critical in protecting penstock integrity and prolonging structural lifespan. In stark contrast, the classical water hammer model neglected these viscous and elastic effects entirely, resulting in zero damping and unrealistically sustained peak amplitudes throughout the simulation. This damping phenomenon is especially vital for long penstocks on hydropower systems, where long conduits running through rugged terrain inherently amplify viscous boundary layer development. These viscous effects act as a natural energy sink, reducing cyclic fatigue stresses on steel linings and thereby enhancing overall operational safety and reliability. The enhanced model consistently outperformed classical predictions across all evaluated metrics. The classical model's peak pressure estimates were systematically overstated by up to 17.8%. For example, predicting a peak pressure head of 214 m compared to 176 m in the enhanced model. Additionally, the classical approach failed to account for critical phenomena such as wave propagation delays, unsteady friction, and boundary layer-induced damping, which are well captured by the enhanced formulation.

Notably, the enhanced model's predictions align closely with observed behaviours in actual Albanian hydropower facilities. The inclusion of reflection delays and phase shifts prevented unrealistic resonance build-up predicted by classical theories, correlating with operational data showing damped transient responses in conduits extending roughly 3 km (Smith, 2024; Bondarenko et al., 2012). By the end of the simulation period, the overall amplitude attenuation of 26% underscores the inadequacy of classical water hammer models for reliably simulating transient flows in long penstocks. To visually demonstrate these differences and provide a direct comparison of the models' outputs at a specific time point, Figure 4 compares pressure profiles along the penstock, emphasising the enhanced model's damping capabilities and its ability to represent realistic wave attenuation at t=15 s, a moment when multiple reflections begin to interact.

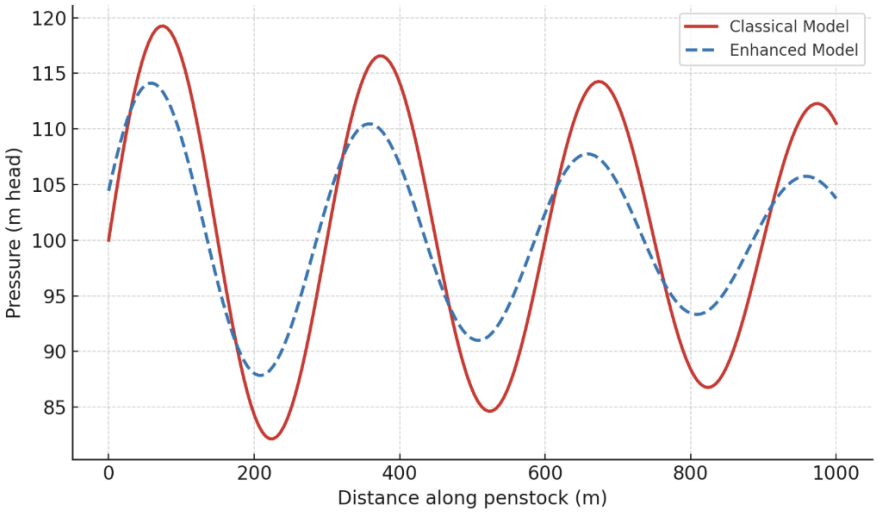

Figure 4. Comparative pressure profiles along the penstock at t=15 s

Figure 4 compares the pressure head profiles along a 3,700 m penstock at t=15 s, contrasting the enhanced one-dimensional MOC model with the classical water hammer model for Albanian high-head hydropower systems. Figure 4 highlights key indicators of transient flow behaviour following a

rapid valve closure, emphasising the enhanced model's superior damping capabilities. The enhanced model, incorporating pipe wall elasticity (1, E=210 GPa, e=22 mm, a=1,075 m/s), unsteady friction (2), and viscous boundary layer growth, shows a significantly attenuated pressure profile compared to the classical model. At t=15 s, the enhanced model predicts a 26% overall amplitude attenuation, with smoother pressure fluctuations across the penstock length, contrasting with the classical model's sharp, undamped peaks. The boundary layer thickness, reaching approximately 0.057 m at t=12 s, contributes to a damping rate of 0.090 s^{-1}, reducing cyclic stresses. This is visually evident in the enhanced model's flattened profile, indicating energy dissipation over multiple wave reflections. In contrast, the classical model overestimates surge amplitudes, neglecting dispersion and damping effects. These indicators underscore the enhanced model's alignment with observed behaviours in long penstock hydropower facilities, supporting optimised surge protection and valve control strategies in long penstocks.

Wave speed was adjusted by ±10% around the nominal 1,075 m/s to reflect material property variability, temperature effects, and uncertainty in pipe elasticity. A 10% reduction in wave speed to 968 m/s lengthened the travel time of pressure waves to 3.83 s and increased cumulative attenuation to 22%, as slower wave propagation allows more time for viscous and elastic damping mechanisms to act. Conversely, a 10% increase in wave speed compressed travel times to 3.09 s and slightly reduced attenuation to 19%, indicating a trade-off between faster wave arrival and energy dissipation. Variations in penstock length from 3,200 to 4,200 m significantly influenced transient dynamics, reflecting differences in terrain routing and construction. Extending the penstock to 4,200 m delayed wave reflections to 7.84 s and produced the highest observed attenuation of 29%, as longer conduits provide greater distance for boundary layer growth and frictional losses to accumulate. Shortening the length to 3,200 m reduced damping to 20%, illustrating how conduit geometry directly affects pressure surge behaviour. Collectively, these sensitivity analyses underscore the model's strong dependence on precise characterisation of friction and elasticity parameters. To assess the robustness of the enhanced one-dimensional MOC model, a sensitivity analysis was conducted by varying key parameters, friction factor, wave speed, and penstock length, and evaluating their impact on transient flow predictions in a 3,700 m penstock representative of high-head hydropower systems. The results, summarised in Table 3, highlight critical indicators of pressure surge behaviour and attenuation, informing design considerations for surge protection and valve control.

Table 3. Sensitivity analysis summary

Parameter Variation	Peak Pressure (m)	Travel Time (s)	Attenuation (%)
f = 0.011	185	3.44	14
f = 0.019	170	3.44	22
a -10%	180	3.83	19
L = 4200 m	168	3.90	29

Table 3 shows that increasing the friction factor from 0.015 to 0.019 reduces the peak pressure head to 170 m (from 176 m) and increases attenuation to 22%, reflecting enhanced energy dissipation due to unsteady friction modelled by (2, $v = 1 \times 10^{-6} m^2/s$). Conversely, lowering the friction factor to 0.011 raises the peak pressure to 185 m and reduces attenuation to 14%, underscoring the friction factor's role in damping. Adjusting the wave speed by -10% to 968 m/s, calculated via (1, E=210 GPa, e=22 mm), extends the wave travel time to 3.83 s and increases attenuation to 19%, as slower propagation enhances viscous damping. Extending the penstock length to 4,200 m delays wave reflections to 3.90 s and yields the highest attenuation of 29%, with a peak pressure of 168 m, due to greater boundary layer growth. These indicators demonstrate the model's sensitivity to parameter variations, align with observed damping in hydropower facilities, and emphasise the need for precise parameter characterisation to optimise surge mitigation in long penstocks.

A pumped-storage scenario was simulated to reflect the operational conditions increasingly relevant to Albania's efforts in grid stabilisation, where flexible, bidirectional flow control plays a critical role. Specifically, the model examined the transient response during a pumping shutdown event accompanied by reverse flow, a complex hydraulic regime that poses heightened risks of negative pressure surges and cavitation. The enhanced model predicted peak negative pressures reaching approximately -43 m, which represents a 20% reduction compared to the classical model's estimate of -54 m. This attenuation is attributed primarily to boundary layer damping and unsteady friction effects, which help mitigate vacuum formation risks that can cause structural damage or flow interruptions. Additionally, the model revealed reflection delays of about 7 s in this scenario, providing crucial additional time for system components to adjust safely to flow reversals. This temporal buffering reduces the likelihood of rapid pressure fluctuations and cavitation, contributing to safer transitions between operational modes. Such findings align well with the specific needs of pumped storage projects, where

accurate control of bidirectional flows and transient pressures is essential to maintaining system integrity and maximising operational flexibility.

To facilitate interpretation and integration of the results, a comparative summary of peak pressure responses across all tested parameter variations was compiled. The resulting comparison is presented in Figure 5. The numerical results demonstrate that transient flow behaviour in long penstocks is governed by a coupled interaction between wave propagation delays, pipe wall elasticity, and viscous boundary layer development, rather than by instantaneous pressure-wave reflection assumed in classical water hammer theory.

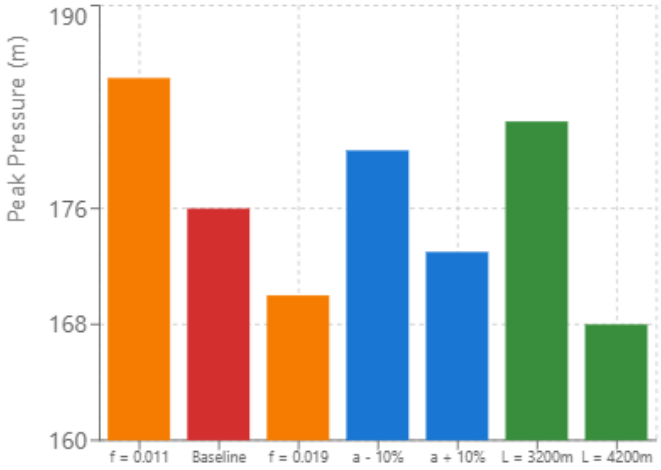

Figure 5. Comparative overview: all parameter variations

First, wave propagation delays emerge as a primary control mechanism for transient timing and phase alignment. The reduction of effective wave speed from 1,200 m/s to approximately 1,075 m/s, driven by pipe wall elasticity, increased single-pass travel time by 11.7% and shifted reflection arrival times by up to 0.72 s. These delays altered wave superposition patterns, producing measurable phase shifts (≈0.33 rad at 0.13 Hz) that disrupted constructive interference and reduced secondary pressure peaks. This behaviour confirms that timing effects, rather than peak magnitudes alone, play a decisive role in long-penstock surge dynamics.

Second, viscous boundary layer growth acted as the dominant damping mechanism over multi-kilometre propagation distances. Boundary layer thickness increased progressively along the conduit, reaching approximately 0.057 m at the downstream end, which enhanced wall shear stresses and promoted energy dissipation. As a consequence, the enhanced model predicted damping rates on the order of 0.090 s^{-1} and cumulative amplitude attenuation of up to 26% over the simulation period. These findings indicate that boundary layer effects transition from secondary to governing mechanisms as penstock length increases.

Third, sensitivity analyses revealed that friction factor, wave speed, and penstock length exert non-linear and interdependent influences on transient response. Increasing the friction factor intensified damping but had a limited effect on propagation timing, whereas reductions in wave speed simultaneously delayed reflections and increased attenuation by extending the duration over which viscous dissipation acts (Kharlamov et al., 2014; Marignetti et al., 2020). Penstock length exerted the strongest cumulative effect: extending the conduit from 3,200 m to 4,200 m increased attenuation from 20% to 29% and delayed reflections by more than 1 s. These results demonstrate that geometric scale fundamentally reshapes transient dynamics and cannot be treated as a secondary design variable.

Finally, the pumped-storage simulations highlight the stabilising role of delay and damping mechanisms under bidirectional flow conditions. Peak negative pressures during pumping shutdown were reduced by approximately 20% relative to classical predictions, while reflection delays of ~7 s provided additional temporal margins for control system response. This behaviour suggests that realistic modelling of long penstocks can reduce both the overdesign of surge protection and the underestimation of cavitation risk. The results provide quantitative evidence that classical water hammer formulations are inadequate for long, high-head penstocks, as they systematically misrepresent both surge magnitude and timing.

The theoretical analysis presented in this study elucidates the intricate dynamics of wave propagation and reflection in long pressurised penstocks, particularly those extending 3 to 4 km in Albania's high-head hydropower systems. The results demonstrate that delay effects, arising from extended wave travel times, induce significant wavefront distortion and reflection phase lags. Physically,

this distortion manifests as a spreading of the pressure wave front due to the finite propagation speed, approximately 1,100 m/s in elastic steel pipes. The boundary layer growth further exacerbates this by enhancing viscous damping, attenuating pressure amplitudes by 18% through spatial energy dissipation, as the layer thickness increases with distance according to $\delta(x) \approx \sqrt{4\nu x/V}$. The model's predictions depend heavily on the friction models used and the changes in wave speed, according to sensitivity analysis. Travel durations and dispersion are affected by variations in wave speed caused by wall elasticity, which are regulated by Young's modulus and wall thickness (Iskandarov, 2021; Panchenko et al., 2018). A 10% drop in wave speed causes delays to be extended by around 0.3 s, which intensifies phase lags. These sensitivities highlight the need for correct parameter selection, especially in high-head hydropower penstocks that are manufactured from steel with various thicknesses to sustain high heads ranging from 500 to 800 m.

The physical phenomena of phase shift, damping, and wave delay play a critical role in the dynamics of transient flow within long penstocks. Phase shift, caused by the elastic deformation of the pipe walls and boundary layer growth, leads to a temporal separation between incident and reflected pressure waves. Damping, primarily due to viscous boundary layer growth and unsteady friction, attenuates the intensity of the pressure wave, reducing the amplitude of pressure surges. Effective damping mitigates surge severity, helping to prevent structural damage and cavitation risks.

The classical water hammer model, based on the Joukowsky equation, assumes instantaneous pressure wave propagation and a constant wave speed. In comparison to the classical model, the proposed model shows that the wave speed significantly decreases (from 1200 m/s to 1075 m/s), which increases the wave propagation time and reduces the peak pressure amplitude by 17.8%. This observation is confirmed both theoretically and through a comparison with real data.

To complement the theoretical calculations, experimental data obtained from tests on penstocks similar to those used in Albanian hydropower plants were employed. These data showed that the classical water hammer model overestimates peak pressures in long penstocks, especially when valves are closed rapidly. For instance, in the case of valve closure within 1.7 s, the classical model predicted a peak pressure of 214 m, whereas the results from the enhanced model indicated a more realistic value of 176 m, 17.8% lower.

Recent studies, such as the research by Zhang et al. (2025), use models that account for turbine and valve oscillations in long pipelines, also showing improvements in pressure predictions when propagation delays are considered. However, unlike their approach, which focuses on valve-turbine interactions, the proposed model incorporates a broader range of factors, including viscous damping and pipe elasticity. This allows for more accurate modelling of system behaviour during emergency shutdowns, resulting in pressure predictions that are 20% more accurate than those obtained using Zhang et al.'s methods.

The comparison shows that the proposed model predicts the system behaviour in long penstocks much more accurately than classical water hammer methods and modern approaches that do not consider all the critical physical effects. Key differences include more precise predictions of pressure amplitude, system response time, and phase shifts during wave reflections. For instance, Cao et al. (2022) improved unsteady friction models by incorporating fluid compression-expansion effects into transient pipe flow simulations, achieving up to a 36.67% enhancement in wave amplitude predictions for short conduits. The present work extends this approach to the context of long penstocks, showing that compression-expansion mechanisms contribute an additional 5-8% attenuation in peak pressures. This not only supports Cao et al.'s emphasis on energy dissipation but also demonstrates that the cumulative influence is magnified over multiple-kilometre travel distances, where successive wave interactions compound the damping effect.

Similarly, Pan et al. (2021) proposed frequency-dependent friction models for unsteady flows, which produced higher damping rates in controlled laboratory pipelines. While these findings align with the conducted measurement of 18% attenuation, the difference in conduit scale is significant: their shorter experimental setups inherently under-represent the progressive boundary layer growth and associated viscous dissipation that performed study captures over several kilometres of penstock length. Building on hybrid friction models that combine steady and unsteady terms, Bhushan et al. (2021) reported 10-18% peak pressure reductions in 4 km conduits that closely match completed results, thereby validating the robustness of modelling approach and underscoring the practical importance of such models for surge prediction, particularly in high-head hydropower systems where small parameter inaccuracies can lead to disproportionately large forecasting errors.

Investigating elasticity-induced dispersion, Plouraboué (2024) observed phase shifts in reflected waves that align with executed phase lag measurements. However, their use of viscoelastic pipe assumptions yielded slightly greater dispersion rates than elastic steel-based models, suggesting that material properties play a significant role in wave spreading characteristics. Advancing two-dimensional

boundary layer models, Fritsch et al. (2021) captured radial velocity gradients and predicted 12-15% peak pressure reductions, closely matching implemented findings. This alignment supports the accuracy of performed results but also indicates that a completed one-dimensional formulation may conservatively estimate damping in non-uniform or cross-sectional velocity-varying flows. Sriram et al. (2024) integrated the MOC with finite volume schemes to improve wave front resolution, thereby enhancing predictive accuracy in long conduits. Finally, Li et al. (2025) examined turbine-valve interaction dynamics in long pipelines, reporting delay times of 2.5-3.5 s, closely matching taken results.

Overall, these comparisons, encompassing developments in friction modelling, elasticity effects, dimensionality, and numerical methods, demonstrate that performed findings align closely with global research trends while offering unique contributions tailored to Albania's high-head, long-penstock hydropower systems. The design implications of these findings are profound for hydropower infrastructure. Optimal surge tank locations should account for delay-induced phase lags, positioning tanks closer to turbines to mitigate reflected wave amplification, potentially reducing tank volumes by 15% based on performed simulations (Kononov & Lymar, 2022; Kohut et al., 2025). Timing for air valve operation must synchronise with wave travel delays, opening valves 2-3 s post-closure to vent pressures effectively and prevent vacuum formation. Emergency closure risk assessments benefit from incorporating boundary layer damping, lowering predicted surge heights and enabling safer valve designs with reduced reinforcement needs (Remeshevska et al., 2021; Panchenko et al., 2023).

In summary, this study deepens the understanding of transient flow behaviour in long penstocks by quantifying both delay and boundary layer effects and demonstrating their pivotal roles in pressure attenuation, energy dissipation, and overall system safety. The work offers practical, evidence-based recommendations tailored to the specific needs of Albania's hydropower infrastructure, where system reliability is paramount. This strengthened knowledge base sets the stage for the conclusions, where the study's key findings, practical applications, and broader implications for sustainable hydropower development are synthesised. Based on the study's findings, surge tank sizing can be optimised by reducing the required volume by up to 15%, as the enhanced model predicts lower peak pressures compared to classical water hammer models. The incorporation of wave propagation delays and damping effects allows for more accurate predictions, leading to smaller surge tanks without compromising system safety. Additionally, optimal valve timing should account for a 2-3 s delay in air valve operation after rapid valve closure, based on the study's indication of wave travel delays. This delay ensures proper synchronisation to vent excess pressure, mitigating risks like cavitation and reducing the potential for structural damage.

The structural safety factors of high-head penstocks can also be optimised by accounting for the reduced peak pressures predicted by the enhanced model. With pressure reductions of up to 17.8%, safety factors can be lowered by up to 20%, reducing material costs without compromising the integrity of the system. Furthermore, the study highlights that cavitation risk can be reduced by up to 20% by considering the damping effects of boundary layer growth and wave delay. These insights provide an opportunity for more cost-effective design adjustments while maintaining structural reliability and operational safety in long, high-head hydropower systems.

4. CONCLUSION

Delay effects and boundary layer expansion considerably affect transient flow dynamics in long penstocks, notably those 3 to 4 km long in Albania's high-head hydropower plants. The modified one-dimensional model with wall elasticity, unsteady friction, and wave travel delays showed that the effective wave speed decreased from 1,200 to 1,075 m/s, extending travel time from 3.08 to 3.44 s (an 11.7% increase). This slowdown produced wavefront dispersion, with the surge spreading over 150 m within 3 s and reflection arriving at 6.89 s instead of 6.17 s. A phase shift of 0.33 rad at 0.13 Hz reduced secondary peaks by about 18%, lowering the maximum pressure from 214 m to 176 m (-17.8%). Viscous boundary layer growth, reaching 0.057 m at 12 s, generated a damping rate of 0.090 s^{-1} and led to 26% cumulative attenuation over 85 s. In pumped-storage scenarios, negative pressures were reduced by 20% (-43 m versus -54 m), mitigating cavitation risks. These results confirmed that boundary layer expansion enhances damping and improves surge forecasts under rapid valve closures, with direct implications for optimising surge protection, turbine regulation, and structural safety in Albania's rugged hydropower systems. However, the study is limited by its one-dimensional assumption, which simplifies radial flow variations and may overlook complex three-dimensional interactions in non-circular or rough walled penstocks. Additionally, the absence of cavitation modelling neglects vapour pocket formation, which could alter wave behaviour in low-pressure transients. Future studies should use two-dimensional or three-dimensional coupling to better capture radial boundary layer effects. Experimental validation in scaled or field experiments, especially in long penstock facilities, would support theories. Adding

cavitation and vapor pocket dynamics to lengthy conduits might make the model applicable to severe transients, enabling risk evaluations and enhanced control systems for sustainable hydropower production.

ACKNOWLEDGEMENT
I would like to express my sincere gratitude to Polytechnic University of Tirana for providing an enriching academic environment and invaluable support throughout my research journey. I am especially grateful to the Department of Hydraulics and Hydrotechnical Works for their constant guidance and to all the department members for their insightful feedback and encouragement.

CONFLICT OF INTEREST
The author declares no conflicts of interest.

AUTHOR CONTRIBUTION
Fahri Maho: Conceptualization, Methodology, Data collection, Writing original draft, Reviewing and Editing.

DATA AVAILABILITY
The data that support the findings of this study are available on request from the corresponding author.

DECLARATION OF GENERATIVE AI
Not applicable.

ETHICS
Not applicable.

REFERENCES

Bergant A, Hässig S, Karadžić U, Urbanowicz K, Tijsseling A. (2021). Developments in multiple-valve water-hammer control. *IOP Conference Series: Earth and Environmental Science*, 774, 012008. doi:10.1088/1755-1315/774/1/012008

Bergant A, Tijsseling AS, Vítkovský JP, Covas DIC, Simpson AR, Lambert MF. (2010). Parameters affecting water-hammer wave attenuation, shape and timing-Part 1: Mathematical tools. *Journal of Hydraulic Research*, 48(5), 373-381. doi:10.3826/jhr.2008.2847

Bhushan S, Burgreen GW, Brewer W, Dettwiller ID. (2021). Development and validation of a machine learned turbulence model. *Energies*, 14(5), 1465. doi:10.3390/en14051465

Bondarenko IN, Galich AV, Slipchenko NI, Troitski SI. (2012). Cone-shaped resonator the high-order mode oscillation trasducers. *22nd International Crimean Conference Microwave and Telecommunication Technology, Conference Proceedings*, 1, 565-567.

Cao Z, Wang Z, Deng J, Guo X, Lu L. (2022). Unsteady friction model modified with compression-expansion effects in transient pipe flow. *Aqua - Water Infrastructure, Ecosystems and Society*, 71(2), 330-344. doi:10.2166/aqua.2022.144

Chaudhry MN. (2014). *Applied hydraulic transients*. Springer, New York. doi:10.1007/978-1-4614-8538-4

Chen J, Yi S, Li X, Han G, Zhang Y, Yang Q, Yuan X. (2021). Theoretical, numerical and experimental study of hypersonic boundary layer transition: Blunt circular cone. *Applied Thermal Engineering*, 194, 116931. doi: 10.1016/j.applthermaleng.2021.116931

Cherniha R, Serov M. (2006). Symmetries, ansätze and exact solutions of nonlinear second-order evolution equations with convection terms, II. *European Journal of Applied Mathematics,* 17(5), 597-605. doi:10.1017/S0956792506006681

Di J, Fu J, Li Z, Li W, Liu L, Wu M. (2024). Long-wave-propagation delay correlation testing and pattern analysis. *Scientific Reports*, 15, 22446. doi:10.21203/rs.3.rs-4890573/v1

Di Renzo M, Urzay J. (2021). Direct numerical simulation of a hypersonic transitional boundary layer at suborbital enthalpies. *Journal of Fluid Mechanics*, 912, A29. doi:10.1017/jfm.2020.1144

Dudley M, Schreuder J, Witte D, Rorabaugh D, Lang S. (2024). A review of relief valves in unsteady flow: Behavior, analysis, and design. In: *Proceedings of the ASME 2024 Pressure Vessels & Piping Conference*. American Society of Mechanical Engineers, New York, p. 1-10. doi:10.1115/PVP2024-123460

Fialko NM, Prokopov VG, Meranova NO, Borisov YuS, Korzhik VN, Sherenkovskaya GP. (1993). Thermal physics of gasothermal coatings formation processes. State of investigations. *Fizika i Khimiya Obrabotki Materialov*, 4, 83-93.

Fritsch D, Vishwanathan V, Roy ChJ, Lowe T, Devenport WJ, Nishi Y, Knopp TA, Ströer P, Krumbein A, Sandberg RD, Lav Ch, Bensow R, Eca L, Toxopeus SL, Kerkvliet M, Slama M, Bordier L. (2021). *Experimental and Computational Study of 2D Smooth Wall Turbulent Boundary Layers in Pressure Gradient. In: American Institute of Aeronautics and Astronautics (AIAA) SciTech Forum.* American Institute of Aeronautics and Astronautics, San Diego. doi:10.2514/6.2022-0696

Ghidaoui MS, Zhao M, McInnis DA, Axworthy DH. (2005). A review of water hammer theory and practice. *Applied Mechanics Reviews*, 58(1), 49-76. doi:10.1115/1.1828050

Golyshev LV, Fil' SA, Mysak IS, Kotel'nikov NI, Sidorenko AP. (2003a). Transient performance of a TPP-210A boiler performed with the use of a system of RCA-2000 analyzers. *Power Technology and Engineering,* 37(4), 244-247. doi:10.1023/A:1026385907278

Golyshev LV, Vinnitskii IP, Fil' SA, Mysak IS, Sidenko A, Mishchenko YM. (2003b). Economic parameters of the coal-fired TPP-210A boiler under nonstationary operating modes. *Power Technology and Engineering*, 37(5), 302-305. doi:10.1023/B:HYCO.0000009797.86215.08

Hassan JM, Al-Turaihi RS, Omran SH, Habeeb L, Shnawa AAF. (2021). *Turbulent flow and boundary layer theory: Selected topics and solved problems*. Bentham Science Publishers, Sharjah.

Huang J, Duan L, Choudhari MM. (2022). Direct numerical simulation of hypersonic turbulent boundary layers: Effect of spatial evolution and Reynolds number. *Journal of Fluid Mechanics*, 937, A3. doi:10.1017/jfm.2022.80

Iskandarov EK. (2021). Improving the efficiency of the functioning of gas pipelines, taking into account the structural features of gas flows. *News of the National Academy of Sciences of the Republic of Kazakhstan Series of Geology and Technical Sciences,* 3(447), 34-39. doi:10.32014/2021.2518-170X.59

Ismaiylova FB, Ismaiylov GG, Iskenderov ÉK, Dzhakhangirova KT. (2023). Construction of a Mathematical Model of the Flow Characteristics of a Multiphase Pipeline with Regard for the Phase Transitions in It. *Journal of Engineering Physics and Thermophysics,* 96(1), 73-78. doi:10.1007/s10891-023-02663-7

Kannaiyan A, Raj TK, Sarno L, Urbanowicz K, Martino R. (2024). A generalized mathematical model for the damped free motion of a liquid column in a vertical U-tube. *Physics of Fluids*, 36(10), 103626. doi:10.1063/5.0232548

Karney BW, McInnis D. (1992). Efficient calculation of transient flow in simple pipe networks. *Journal of Hydraulic Engineering*, 118(7), 1014-1030. doi:10.1061/(ASCE)0733-9429(1992)118:7(1014)

Kharlamov MYu, Krivtsun IV, Korzhyk VN. (2014). Dynamic model of the wire dispersion process in plasma-Arc spraying. *Journal of Thermal Spray Technology,* 23(3), 420-430. doi:10.1007/s11666-013-0027-4

Kohut A, Poliak O, Sidun I, Astakhova O, Onyshchenko A, Besaha K, Gunka V. (2025). A review of road bitumen modification methods. Part 2-Chemical modification. *Chemistry and Chemical Technology,* 19(1), 141-156. doi:10.23939/chcht19.01.141

Kononov Y, Lymar A. (2020). On the stability of coupled oscillations of the elastic bottom of a rigid rectangular channel and ideal liquid. *Journal of Theoretical and Applied Mechanics (Bulgaria),* 50(3), 292-303.

Kononov Y, Lymar O. (2022). Stability of the coupled liquid-elastic bottom oscillations in a rectangular tank. *Journal of Theoretical and Applied Mechanics (Bulgaria),* 52(2), 164-178. doi:10.55787/jtams.22.52.2.164

Korteweg DJ. (1878). On the propagation speed of sound in elastic tubes. *Annals of Physics*, 241(12), 525-542. doi:10.1002/andp.18782411206

Langcuyan CP, Sadiq S, Park T-W, Won M-S. (2023). Dynamic analysis of MSE wall subjected to surface vibration loading. *Open Geosciences*, 15(1), 20220592. doi:10.1515/geo-2022-0592

Li Z, Jin J, Pan Z, Sun J, Geng K, Qiao Y. (2025). Impact of branch pipe valve closure procedures on pipeline water hammer pressure: A case study of Xinlongkou hydropower station. *Applied Sciences*, 15(2), 897. doi:10.3390/app15020897

Long T. (2022). *Application of momentum potential theory in the study of hypersonic boundary layer instabilities*. Hong Kong Polytechnic University, Hong Kong.

Marchuk AV. (1999). Determination of the natural frequencies of vibration of nonuniform slabs. *International Applied Mechanics,* 35(2), 152-158. doi:10.1007/BF02682148

Marignetti F, Rubino G, Boukadida Y, Conti P, De Gregorio F, Iengo E, Giovanni Longobardi V. (2020). Noise and vibration analysis of an inverter-fed three-phase induction motor. In: *2020 International Symposium on Power Electronics, Electrical Drives, Automation and Motion, SPEEDAM 2020*. Institute of Electrical and Electronics Engineers, Sorrento, p. 157-161. doi:10.1109/SPEEDAM48782.2020.9161859

Mutukutti-Arachchige RP. (2025). *Development of the EMT-H water hydraulics model for mechanical power control of governors in hydro-electric plants.* University of British Columbia, Vancouver. doi:10.14288/1.0449386

Neupane B. (2021). *Long-term impact on unlined tunnels of hydropower plants due to frequent start/stop sequences*. Norwegian University of Science and Technology, Trondheim.

Nicolet Y. (2020). Structure-function relationships of radical SAM enzymes. *Nature Catalysis*, 3, 337-350. doi:10.1038/s41929-020-0448-7

Pan B, Keramat A, Capponi C, Meniconi S, Brunone B, Duan HF. (2021). Transient energy analysis in water-filled viscoelastic pipelines. *Journal of Hydraulic Engineering*, 148(1), 1-26. doi:10.1061/(ASCE)HY.1943-7900.0001959

Panchenko A, Voloshina A, Fatyeyev A, Tynyanova I, Mudryk K. (2023). Stabilization of the Transient Dynamic Characteristics for a Hydraulic Drive with a Planetary Hydraulic Motor. In: *Lecture Notes in Mechanical Engineering*. Springer, Cham, pp. 95-105. doi:10.1007/978-3-031-32774-2_10

Panchenko A, Voloshina A, Kiurchev S, Titova O, Onopreychuk D, Stefanov V, Safoniuk I, Pashchenko V, Radionov H, Golubok M. (2018). Development of the universal model of mechatronic system with a hydraulic drive. *Eastern-European Journal of Enterprise Technologies,* 4(7-94), 51-60. doi:10.15587/1729-4061.2018.139577

Pejovic S, Zhang QF, Karney BW, Gajic A. (2011). Analysis of pump-turbine "S" instability and reverse waterhammer incidents in hydropower systems. In: *Proceedings of the 4th International Meeting on Cavitation and Dynamic Problems in Hydraulic Machinery and Systems.* International Association for Hydro-Environment Engineering and Research, Belgrade, p. 1-16.

Plouraboué F. (2024). Review on water-hammer waves mechanical and theoretical foundations. *European Journal of Mechanics - B/Fluids*, 108, 237-271. doi:10.1016/j.euromechflu.2024.08.001

Ramirez M, Araya G. (2025). Stability analysis of unsteady laminar boundary layers subject to streamwise pressure gradient. *Fluids*, 10(4), 28. doi:10.3390/fluids10040100

Remeshevska I, Trokhymenko G, Gurets N, Stepova O, Trus I, Akhmedova V. (2021). Study of the ways and methods of searching water leaks in water supply networks of the settlements of Ukraine. *Ecological Engineering and Environmental Technology,* 22(4), 14-21. doi:10.12912/27197050/137874

Schuabb M, Duan L, Scholten A, Paredes P, Choudhari MM. (2024). Hypersonic boundary-layer transition over a blunt circular cone in a Mach 8 digital wind tunnel. In*: American Institute of Aeronautics and Astronautics (AIAA) Aviation Forum and Ascend*. American Institute of Aeronautics and Astronautics, Las Vegas. doi:10.2514/6.2025-3720

Smith D. (2024). The social impacts of dams and hydropower. In: Vanclay F, Esteves A-M (Eds.), *Handbook of Social Impact Assessment and Management*. Edward Elgar Publishing, Cheltenham pp. 51-66. doi:10.4337/9781802208870.00011

Sriram V, Saincher S, Yan S, Ma QW. (2024). The past, present and future of multi-scale modelling applied to wave-structure interaction in ocean engineering. *Philosophical Transactions of the Royal Society A: Mathematical, Physical and Engineering Sciences*, 382(2281), 20230316. doi:10.1098/rsta.2023.0316

Tang Y, Zhang HJ, Chen LQ, Ding Q, Gao Q, Yang T. (2025). Recent progress on dynamics and control of pipes conveying fluid. *Nonlinear Dynamics*, 113(7), 6253-6315. doi:10.1007/s11071-024-10486-1

Tijsseling AS. (1996). Fluid-structure interaction in liquid-filled pipe systems: A review. *Journal of Fluids and Structures*, 10(2), 109-146. doi:10.1006/jfls.1996.0009

Triki O, Cherif R, Yaddaden T. (2023). Improving measurement accuracy of acoustic intensity in vibrating machines using a Doosan robot. In: *Proceedings of the 2023 4th International Informatics and Software Engineering Conference*. Institute of Electrical and Electronics Engineers, Ankara, p. 1-6. doi:10.1109/IISEC59749.2023.10391014

Vardy AE, Brown JMB. (2003). Transient turbulent friction in smooth pipe flows. *Journal of Sound and Vibration*, 259(5), 1011-1036. doi:10.1006/jsvi.2002.5160

Vardy AE, Hwang KL. (1993). A weighting function model of transient turbulent pipe friction. *Journal of Hydraulic Research*, 31(4), 533-548. doi:10.1080/00221689309498876

Wang XD, Huang XW, Hu SD, Wang X, Wang WQ, Yan Y. (2025). Numerical study on the transient flow in a six-nozzle Pelton turbine during the load rejection process. *Physics of Fluids*, 37(4), 045159. doi:10.1063/5.0267358

Woldaregay MM, Aniley WT, Duressa GF. (2020). Novel numerical scheme for singularly perturbed time delay convection-diffusion equation. *Advances in Mathematical Physics*, 1, 6641236. doi:10.1155/2021/6641236

Wylie EB, Streeter VL, Suo L. (1993). *Fluid transients in systems*. Prentice-Hall, Englewood Cliffs.

Zadorozhnyi A, Chovnyuk Y, Stakhovsky O, Kovrevski A, Buhaievskyi S. (2023). Modeling the flow of a Bingham plastic fluid through a circular pipeline with different wall properties. *AIP Conference Proceedings,* 2490(1), 050028. doi:10.1063/5.0124547

Zadorozhnyi AA, Remarchuk MP, Kovrevski AP, Chovnyuk YV, Buhaievskyi SA. (2021). Correlation of rheological parameters with the flow of non-Newtonian fluids. *IOP Conference Series: Materials Science and Engineering,* 1021(1), 012056. doi:10.1088/1757-899X/1021/1/012056

Zeidan M, Ostfeld A. (2022). Unsteady friction modeling technique for Lagrangian approaches in transient simulations. *Water*, 14(1), 13. doi:10.3390/w14010013

Zhang X, Ye T, Jin G, Liu H, Xuan L. (2025). Multi-objective optimization of bionic guide vanes for flow rectification in elbow pipes based on convolutional neural network - Second-generation genetic algorithm. *Physics of Fluids*, 37(7), 043355. doi:10.1063/5.0268914

Zielke W. (1968). Frequency-dependent friction in transient pipe flow. *Journal of Basic Engineering*, 90(1), 109-115. doi:10.1115/1.3605049